Modulation-doped-semiconductorlike behavior manifested in magnetotransport measurements of Li_xZrNCl layered superconductors

T. Takano,[1] A. Kitora,[1] Y. Taguchi,[1,2] and Y. Iwasa[1,2]
[1]*Institute for Materials Research, Tohoku University, Sendai 980-8577, Japan*
[2]*CREST, Japan Science and Technology Corporation, Kawaguchi 332-0012, Japan*
(Received 7 September 2007; revised manuscript received 21 October 2007; published 18 March 2008)

Transport properties in magnetic fields have been investigated for possibly exotic Li_xZrNCl superconductors with a wide range of doping concentration of $0.06 \leqslant x \leqslant 0.37$. Application of magnetic field along c axis rapidly suppressed the superconducting transition temperature (T_c) while strongly broadening the width. Zero-temperature limit of upper critical field [$H_{c2}(0)$] showed systematic and monotonic decrease upon increasing x. Detailed analysis with a phenomenological argument gave a simple relation of $k_F L \propto x$ and almost x-independent μ (k_F, L, and μ denote Fermi wave number, mean free path, and carrier mobility, respectively). These results combined with the temperature-independent Hall coefficient clearly indicate that the present system can be viewed as modulation-doped semiconductors in which conduction electrons suffer from minimal disorder scattering. This could be a key to the relatively high-T_c values realized in this class of layered superconductors.

DOI: 10.1103/PhysRevB.77.104518 PACS number(s): 74.25.Fy, 74.70.−b, 74.78.Fk

I. INTRODUCTION

Superconductivity is often induced by carrier doping into an insulator, which can be either band insulator or Mott insulator (with strong electron correlation). In the case of a band insulator, the electronic properties of the doped system can be accurately predicted because the independent electron approximation works well. Examples of such superconductors are electron-doped $SrTiO_3$ and hole-doped diamond.[1] On the other hand, although it is more difficult to make a precise prediction about the electronic properties of doped Mott insulators, high-T_c superconductivity can be anticipated, for example, in cuprates, due to the large energy scale of the relevant interaction. In both cases, however, the random distribution of the dopants has significant influence on the T_c values; in the B-doped diamond, it is theoretically pointed out[2] that T_c values are severely limited by the random distribution of B ions over the conduction path. Also, in the cuprates, the disorder in the adjacent plane to the conduction plane has experimentally been reported to reduce the T_c values.[3] One useful way to minimize the disorder effects in doped materials is to exploit the modulation doping technique as extensively adopted in semiconductor physics. The Li-intercalated ZrNCl superconductors treated in this study and its Hf analogs belong to a class of materials in which the electronic properties are predicted by band calculations rather precisely, and also moderately high-T_c values (15 and 25.5 K, respectively) are realized possibly due to collective charge fluctuation, namely, the electron correlation effect. In addition, the T_c values in the Li_xZrNCl system seem to be rather unaffected by the disorder effects, and this would be a consequence of the resemblance to the modulation-doped semiconductors as will be shown in the present paper.

Pristine β-ZrNCl and β-HfNCl are band insulators and have layered structures in which double-honeycomb $[ZrN]_2$ (or $[HfN]_2$) and Cl_2 layers stack alternately along c axis. These materials become superconductors[4,5] upon electron doping by means of Li intercalation. Recent band calculations[6–10] predict highly two-dimensional conduction band consisting of Zr $4d$ (or Hf $5d$) orbitals hybridized with N $2p$ states. Such two dimensionality of the electronic state has experimentally been confirmed by several experiments.[11–14] Since Li ions are accommodated in between the Cl_2 layers, as schematically shown in Fig. 1(a), the two-dimensional electronic system confined in the $[ZrN]_2$ double layers is expected to be little affected by the disorder effect of the Li ions.

The unique feature of these superconductors is dichotomous behavior concerning the coupling strength. On one hand, the electronic density of state at the Fermi level [$N(0)$] is very small for their T_c values, as evidenced by the Pauli paramagnetic susceptibility[15] as well as the normal-state Sommerfeld constant.[16] The observed values are very close to the calculated ones, and therefore, the deduced electron-phonon coupling constant is very small to reproduce the observed value of T_c.[15,16] On the other hand, large values of superconducting gap ratio $2\Delta/k_B T_c$ have been reported.[16,17] Muon spin rotation measurements[13,18] also indicated the

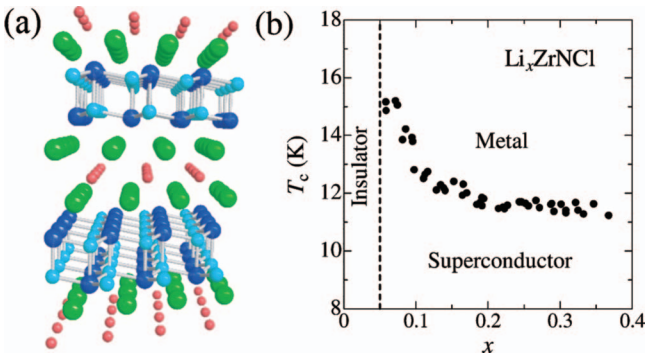

FIG. 1. (Color) (a) A crystal structure of Li_xZrNCl is schematically shown. Red, light blue, blue, and green spheres represent Li, Zr, N, and Cl atoms, respectively. (b) Carrier concentration dependence of superconducting critical temperature (T_c) of a series of Li_xZrNCl.

strong-coupling nature. To explain these apparently contradicting observations, charge fluctuation has been proposed[19] to contribute to the pairing interaction in addition to the phonon and enhances the T_c that would otherwise be much lower.

Recently, we have successfully established a way to obtain single phase samples with controlled doping levels,[20] offering an opportunity to investigate the systematic doping evolution of various electronic properties. One of our findings was that the highest T_c is encountered on the verge of the transition to the insulator, implying that the disorder effect on the T_c is rather weak in this system. In this paper, we report on the systematic resistivity measurements under magnetic fields, including Hall effect, on a wide Li concentration range of $0.06 \leqslant x \leqslant 0.37$. The analysis of the data has revealed that the intrinsic mean free path is rather long and that the mobility is almost independent of the carrier density. These results combined with the temperature-independent Hall coefficients are clear experimental evidence that the transport properties in the Li_xZrNCl superconductor are very similar to those observed in the two-dimensional electron gas in the modulation-doped semiconductor structures. The minimal disorder scattering that the conduction electrons in such a structure suffer from would be important for the realization of relatively high-T_c values in this class of layered nitride superconductors.

II. EXPERIMENT AND SAMPLE CHARACTERIZATION

Details of the sample preparation have already been published in Ref. 20. All the samples investigated in this study were confirmed to be of single phase by means of powder x-ray diffraction experiments performed at BL02B2, SPring-8. The actual Li concentration (x) in the products was determined within an accuracy of ± 0.01 by inductively coupled plasma spectroscopy at analytical research core for advanced materials, IMR, Tohoku University, and thus determined x values are used throughout the paper. The T_c values of all the samples synthesized thus far, including those used for the present transport measurements, have been determined by the magnetization measurements and are plotted as a function of x in Fig. 1(b).

For the resistivity and Hall effect measurements, we prepared c-axis oriented, compressed pellets. Conventional four- and five-probe methods are adopted for resistivity and Hall effect measurements, respectively, with current flowing parallel to the ab plane and with magnetic field applied along c axis. In the Hall effect measurements, we changed the magnetic field from 9 to -9 T by every 1 T and eliminated the magnetoresistance due to the residual longitudinal component which is even with respect to the field reversal.

In order to compare the typical size of the grains in the used polycrystalline samples with the characteristic length scales derived from the transport data, we have taken scanning electron microscopy (SEM) images of the sample surface of the several pellets. The images of $x=0.10$ and 0.35 samples are displayed in Figs. 2(a) and 2(b), respectively, as representatives of lightly and heavily doped samples. Hexagonal-like facet structures reflecting the honeycomb lattice are clearly observed. The typical size of the grain along lateral direction in the SEM images (i.e., along the conduction plane) was found to be several microns, irrespective of the Li concentration x.

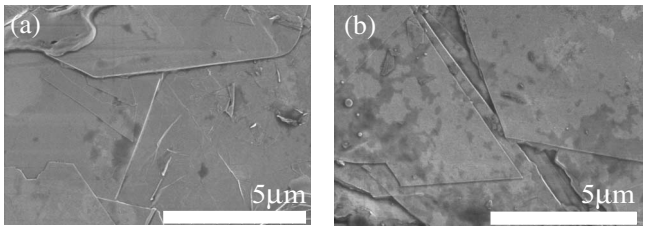

FIG. 2. SEM images of the surface of the compressed pellets for (a) $x=0.10$ and (b) $x=0.35$.

Also, we have checked the grain size by analyzing the width of (110) x-ray diffraction peak of the samples. We determined the grain size of the pristine ZrNCl to be about 2.5 μm from the (110) peak width, taking into account the width arising from the finite resolution which is estimated from the width of standard samples, such as CeO_2 and diamond powder. For the doped samples, we have observed slightly broadened (110) peak as compared with the pristine material. For instance, the exactly same analysis for $x=0.16$ sample gave 0.40 μm as (the lowest limit of) the grain size. However, very similar sizes of the grains in the SEM images of pristine and doped materials (SEM image of the pristine material not shown here) strongly indicate that the apparent broadening observed for the doped sample would be due to the slight distribution of the lattice constants arising from the Li inhomogenity, which is absent in the undoped material, but should be inevitable in the fractionally intercalated materials. In fact, the broadened width of the doped samples can fully be explained if we assume, without any reduction of the grain size, only the inhomogeneous distribution of lattice constant corresponding to that of Li by a tiny amount of ± 0.007 within the sample, which we think is very probable. The extensive characterizations based on both the SEM images and x-ray diffraction peak width consistently indicate that the typical size of the grains is several microns, which is almost 2 orders of magnitude larger than the obtained characteristic length within the conduction plane, such as mean free path of the carriers [see Fig. 5(b)]. Even if we take the lowest limit of the grain size for the doped samples deduced through the analysis of the x-ray peak width, it is still 1 order of magnitude larger than the relevant length scales. On the basis of these considerations, we can safely conclude that the grain boundary effect along the conduction plane is not dominant in the superconducting properties of the present material.

Since the grain size along the direction perpendicular to the surface (i.e., along the c axis) cannot be known from the SEM images, we also collected a diffraction pattern of the powdered sample used for the resistivity measurement with the use of x-ray source ($\lambda=1.54056$ Å) available at laboratory. From the width of (003) peak, we obtained 130 Å as the structural coherence length along the c axis. It should be noted, however, that this value is the lowest limit of the c-axis grain size because of the reduced resolution of the

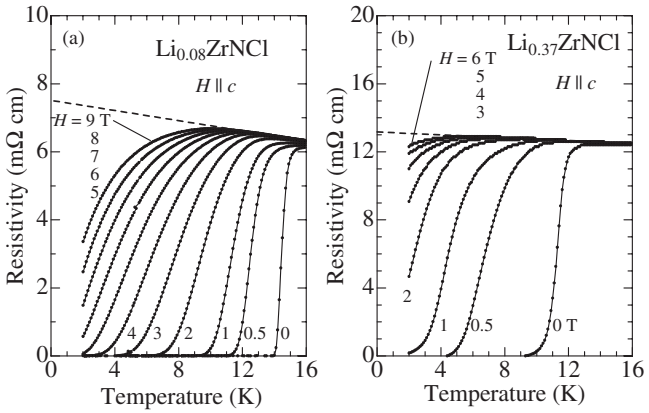

FIG. 3. Temperature dependence of resistivity below 16 K for (a) $Li_{0.08}ZrNCl$ and (b) $Li_{0.37}ZrNCl$ samples in various magnetic fields which were applied perpendicular to the pellets. Dashed lines represent the extrapolation of normal-state resistivity.

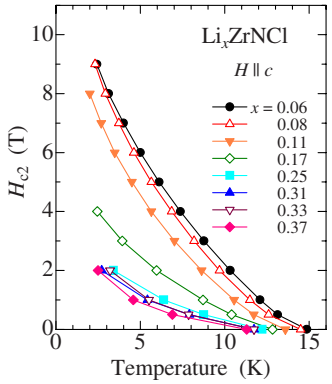

FIG. 4. (Color online) H_{c2}-T phase diagram of Li_xZrNCl samples with various values of x with $H \parallel c$ configuration. In the determination of the phase diagram, we defined $T_c(H)$ as the temperature at which resistivity value decreases to 50% of the normal-state resistivity in a magnetic field H.

diffraction experiment achieved in the laboratory apparatus, and the coherence length of the lattice would actually be longer. Also, comparison of the widths of the (003) peak before and after the pelletization indicated essentially no broadening upon the pelletization. The obtained value of 130 Å, the lowest limit of the grain size along the c axis, is still much longer than the reported value of the c-axis superconducting coherence length (=16 Å) in a very similar material ($ZrNCl_{0.7}$),[14] again indicating that the finite grain size effect along the c axis does not give significant influence upon the superconducting properties.

III. RESISTIVITY MEASUREMENT IN MAGNETIC FIELDS

Figures 3(a) and 3(b) show the temperature dependence of resistivity in various magnetic fields for x=0.08 and 0.37 samples, respectively. The x=0.08 sample shows a rather sharp resistivity drop associated with the superconducting transition at 14–15 K in zero field, and the application of magnetic field reduces T_c while broadening the width of the transition. Such a broadening of the transition width in high magnetic fields has been observed in previous studies,[13,14] and it is characteristic feature of the two-dimensional superconductor. Even in the highest magnetic field (=9 T) of the present study, the resistivity begins to decrease at about 9 K and reaches almost half of the normal-state resistivity value. However, the apparent decrease of the resistivity at low temperatures is ascribed to the fact that there are some misoriented grains in which H is parallel to the ab plane and thus the superconductivity tends to survive. As the Li concentration is increased from 0.08 to 0.37, T_c in zero field is significantly reduced to 11–12 K in accord with the previous result,[20] as clearly seen in Fig. 3(b). More importantly, the magnetic field suppresses the superconductivity more rapidly than in the case of x=0.08 sample. Application of 6 T almost completely suppresses the decrease of the resistivity.

To discuss the doping variation of the H_{c2}-T phase diagram, we plotted in Fig. 4 the T_c values in applied fields for all the investigated samples. It is difficult to determine the T_c values in high magnetic fields because of the broadened resistive transition, but for the analysis, we defined T_c as the temperature at which the resistivity value becomes half of the normal-state resistivity which is represented by dashed lines in Figs. 3(a) and 3(b), for example. As the doping concentration is increased, both zero-field T_c values and $H_{c2}(T)$ decrease systematically. For all the samples, the absolute value of the slope $|\frac{dH_{c2}(T)}{dT}|$ becomes large as the temperature is reduced in accord with the previous results.[13,14] However, this behavior is not an intrinsic property of the present system, but it is merely an artifact arising from the misoriented grains in the compressed pellets used in the present study; most of the grains are aligned in such a way that c axis is parallel to the applied field, but there are some grains in which applied field is within the ab plane. In the $H \parallel ab$ configuration, H_{c2} is larger than in $H \parallel c$ configuration,[14] and therefore superconducting path consisting of $H \parallel ab$ grains survives while most of the grains become normal metal in the high-field region. This is evidenced by the fact that the increasing trend of $|\frac{dH_{c2}(T)}{dT}|$ apparently becomes less conspicuous when the thickness of the pellet for the measurements becomes thinner and hence the degree of orientation of the grains becomes higher.[21]

IV. DOPING DEPENDENCE OF $H_{c2}(0)$ AND RELATED PHYSICAL PARAMETERS

Because of the uncertainty of the $H_{c2}(T)$ values in the low temperature region, we estimated the $T \rightarrow 0$ limit of $H_{c2}(T)$ on the basis of the Werthamer-Helfand-Hohenberg relation,[22] namely, $H_{c2}(0)=0.7T_c|\frac{dH_{c2}}{dT}|_{T=T_c}$, using the data near T_c. Thus, determined $H_{c2}(0)$ values are plotted in Fig. 5(a) as a function of x. H_{c2} value rapidly and monotonically decreases as the doping proceeds. This behavior is in striking contrast to the doping dependence of T_c plotted in Fig. 1(b) which shows little variation in the region of $0.12 \leqslant x \leqslant 0.37$. By using a relation of $H_{c2}(0)=\Phi_0/2\pi\xi^2$, we can obtain the x dependence of coherence length ξ. Here, Φ_0 denotes mag-

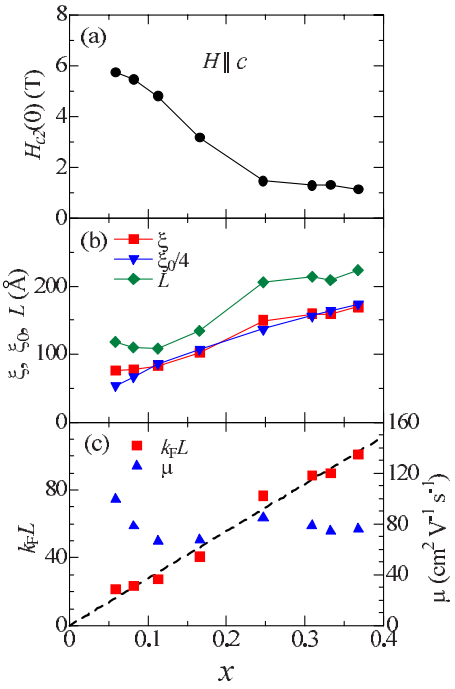

FIG. 5. (Color online) Carrier concentration dependence of (a) $T \to 0$ limit value of H_{c2}, (b) coherence length ξ, the Pippard coherence length ξ_0, mean free path L, and (c) $k_F L$ and carrier mobility μ.

netic flux quantum. The coherence length, in its turn, systematically increases as the carrier concentration is increased, as plotted in Fig. 5(b). To compare this quantity with the Pippard coherence length ξ_0, we calculated ξ_0 by using a relation $\xi_0 = \frac{\hbar v_F}{\pi \Delta} = \frac{\hbar^2 k_F}{2.45 \pi m^* k_B T_c}$, where v_F, Δ, and m^* represent the Fermi velocity, superconducting gap, and effective mass of electrons, respectively. Also, we assumed that a relation of $\frac{2\Delta}{k_B T_c} = 4.9$ which was found for $x = 0.12$ sample in the specific heat measurement[16] holds for all the samples investigated here. For the effective mass of the carriers, we used a value of $m^*/m_0 = 0.66$ which was predicted by a recent band calculation.[10] We calculated k_F by assuming that the Fermi surface is of cylindrical shape. Thus, estimated values of ξ_0 (multiplied by 1/4) are plotted as a function of x also in Fig. 5(b). It is readily noted that ξ is always shorter than ξ_0, but both quantities exhibit very similar doping dependence ($\xi \approx \xi_0/4$). In general, a phenomenological relation of $\frac{1}{\xi} = \frac{1}{\xi_0} + \frac{1}{L}$ holds among ξ, ξ_0, and L. By using this equation, we can obtain doping dependence of L, which is plotted in Fig. 5(b). This quantity also shows an increase as the doping concentration is increased. We further calculated $k_F L$ from thus obtained L and k_F and plotted this quantity as a function of x in Fig. 5(c). Clearly, $k_F L$ increases linearly with increasing x and the data can be fitted to an equation of $k_F L = 280x$. In a two-dimensional system, the resistivity ρ is expressed as $\rho = \frac{\rho_M}{k_F L}$, where $\rho_M = \left(\frac{h}{e^2}\right) d$ (~ 2.4 mΩ cm) is the resistivity at the Ioffe-Regel limit and d (~ 9.3 Å) represents the interplane distance. Using the above result, we obtain an empirical relation of $\rho = \frac{8.6}{x}$ ($\mu\Omega$ cm) as the intrinsic value of the residual resistivity for a series of Li_xZrNCl materials.

This relation indicates that the resistivity values that were actually measured for the compressed pellet seems to be 2 orders of magnitude larger than the genuine values of the material, and the discrepancy should be attributed to the effect of grain boundaries. However, the determination of $H_{c2}(0)$ values is not influenced by the effects of the grain boundaries as they were derived not from the absolute values of the resistivity but from the relative change of ρ against magnetic field. Also, the derived values of ξ (~ 150 Å), ξ_0 (~ 600 Å), and L (~ 250 Å) are much smaller than the typical size of the grains (approximately several microns), ruling out the possibility that the grain boundary effect dominates the $H_{c2}(0)$. Based on these considerations, we conclude that the grain boundary effect gives little influence on the results of the present analysis.

From the obtained values of L, we also calculated the carrier mobility $\mu = \frac{e\tau}{m^*} = \frac{eL}{m^* v_F} = \frac{eL}{\hbar k_F}$, and plotted in Fig. 5(c). The estimated μ is between 65 and 110 (cm^2/V s) and does not show any strong doping dependence, and hence it can be considered to be independent of the carrier concentration. In the present superconductor, Li ions are intercalated in between adjacent Cl layers, and the $[ZrN]_2$ conduction layer, or the stacking unit of Cl-$[ZrN]_2$-Cl layer remains totally intact upon the Li intercalation. The situation can be viewed as a kind of modulation-doping technique adopted in semiconductor quantum well structures. In such systems, it has been established that the mobility μ (due to the ionized impurity scattering) increases, or remains constant, upon increasing the carrier density[23] in the form of $\mu \propto x^\gamma$ once carriers are sufficiently doped to form degenerate state, where γ is theoretically 0.5, but is empirically known to take some value between 0 and 0.5. In particular, the thickness of "spacer layer" becomes thinner, and the γ value becomes smaller. Therefore, the present material can be regarded as a modulation-doped semiconductor (band insulator) with the zero limit of spacer layer thickness. The doping dependence of μ in the Li_xZrNCl system is quite contrastive with the case of $La_{2-x}Sr_xCuO_4$,[24] in which an increase in μ by a factor larger than 3 was observed when the hole concentration x is increased from 0.05 to 0.2. The enhancement of μ would arise from the filling-dependent renormalization of correlation effect in the doped Mott insulator.

V. HALL EFFECT

In Fig. 6(a), we show the resistivity data of the four samples that are used for the Hall effect measurements. The $x = 0.07$ sample shows insulating temperature dependence of resistivity, but other materials exhibit metallic resistivity except for weak localization behavior at low temperatures below approximately 50 K. All the samples show superconducting transition at low temperatures.

In Fig. 6(b), the Hall coefficients (R_H) of these materials are plotted against temperature. The R_H of all the samples are negative, indicating that the doped carriers are of electron type. The notable feature is that R_H is almost temperature independent as in the case of simple metals, making marked contrast with the case of cuprate superconductors,[25,26] except

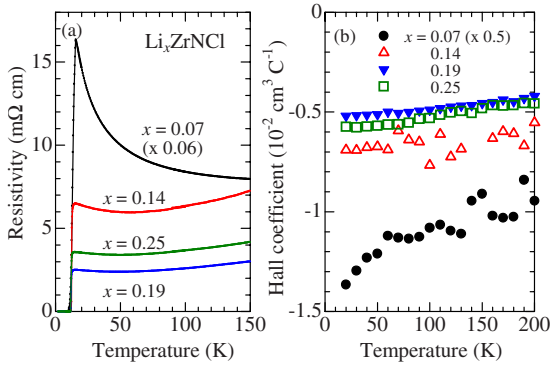

FIG. 6. (Color online) (a) Temperature dependence of resistivity of the samples used for Hall effect measurement. (b) Temperature dependence of the Hall coefficient of four Li_xZrNCl samples.

for $x=0.07$ sample that strongly suffers the effect of localization. This is in accord with the fact that the present superconductor is a single band system when the doping concentration is not very high.[6–10] More importantly, this fact strongly suggests that the scattering rate of the electron is independent of the wave vector on the cylindrical Fermi surface. Therefore, it would be possible to understand the electronic properties of the present system in the normal state on the basis of conventional band theory.

One problem concerning R_H is its magnitude; the absolute value of the observed R_H is three to seven times larger than that expected from a simple relation of $R_H=-\frac{1}{xe}$. It is very probable that this discrepancy in absolute values also arises from the fact that the samples used for the measurements are compressed pellets with grain boundaries. Gigantic enhancement of R_H up to 3 orders of magnitude has been reported[27] in granular Cu-SiO_2 film system, and it has been ascribed to the presence of substructures associated with the grains. Therefore, we interpret the discrepancy in the absolute value of R_H as being extrinsic.

VI. SUMMARY

We investigated the systematic doping evolution of the transport properties in magnetic fields for a series of Li_xZrNCl superconductors with a wide range of doping concentration $0.06 \leqslant x \leqslant 0.37$. Despite using compaction pellet samples, the systematic experiments and the phenomenological consideration allowed us to extract intrinsic transport properties of the present superconductors. As the doping concentration was increased, the $T \rightarrow 0$ limit of upper critical field $[H_{c2}(0)]$ for $H \| c$ configuration systematically and monotonically decreased. From the analysis, we found that the intrinsic mean free path L satisfies a simple relation of $k_F L = 280x$ and the mobility is almost independent of x. Furthermore, the Hall coefficient was found to be almost temperature independent, implying the isotropic scattering rate of the doped carriers. These results show that the transport properties in the Li_xZrNCl superconductor are understood within a scheme of modulation-doped semiconductors. The minimal disorder effects on the conduction electrons must play one of the important roles in producing high-T_c values.

ACKNOWLEDGMENTS

We would like to acknowledge H. Tou, T. Sasaki, and T. Arima for useful discussions and comments. This work was supported in part by a Grant-in-Aid for Scientific Research from MEXT, Japan and by the Nano-Material Developing Project of IMR, Tohoku University. Synchrotron x-ray diffraction measurements were performed at BL02B2, SPring-8 with the approval of JASRI. Magnetization measurements were carried out in part at the Center for Low-Temperature Science, Tohoku University.

[1] E. A. Ekimov, V. A. Sidorov, E. D. Bauer, N. N. Mel'nik, N. J. Curro, J. D. Thompson, and S. M. Stishov, Nature (London) **428**, 542 (2004).
[2] T. Shirakawa, S. Horiuchi, Y. Ohta, and H. Fukuyama, J. Phys. Soc. Jpn. **76**, 014711 (2007).
[3] K. Fujita, T. Noda, K. M. Kojima, H. Eisaki, and S. Uchida, Phys. Rev. Lett. **95**, 097006 (2005).
[4] S. Yamanaka, H. Kawaji, K. Hotehama, and M. Ohashi, Adv. Mater. (Weinheim, Ger.) **8**, 771 (1996).
[5] S. Yamanaka, K. Hotehama, and H. Kawaji, Nature (London) **392**, 580 (1998).
[6] R. Weht, A. Filippetti, and W. E. Pickett, Europhys. Lett. **48**, 320 (1999).
[7] I. Hase and Y. Nishihara, Phys. Rev. B **60**, 1573 (1999).
[8] C. Felser and R. Seshadri, J. Mater. Chem. **9**, 459 (1999).
[9] H. Sugimoto and T. Oguchi, J. Phys. Soc. Jpn. **3**, 2771 (2004).
[10] R. Heid and K.-P. Bohnen, Phys. Rev. B **72**, 134527 (2005).
[11] H. Tou, Y. Maniwa, T. Koiwasaki, and S. Yamanaka, Phys. Rev. B **63**, 020508(R) (2000).
[12] T. Yokoya, Y. Ishiwata, S. Shin, S. Shamoto, K. Iizawa, T. Kajitani, I. Hase, and T. Takahashi, Phys. Rev. B **64**, 153107 (2001).
[13] T. Ito, Y. Fudamoto, A. Fukaya, I. M. Gat-Malureanu, M. I. Larkin, P. L. Russo, A. Savici, Y. J. Uemura, K. Groves, R. Breslow, K. Hotehama, S. Yamanaka, P. Kyriakou, M. Rovers, G. M. Luke, and K. M. Kojima, Phys. Rev. B **69**, 134522 (2004).
[14] H. Tou, Y. J. Tanaka, M. Sera, Y. Taguchi, T. Sasaki, Y. Iwasa, L. Zhu, and S. Yamanaka, Phys. Rev. B **72**, 020501(R) (2005).
[15] H. Tou, Y. Maniwa, T. Koiwasaki, and S. Yamanaka, Phys. Rev. Lett. **86**, 5775 (2001).
[16] Y. Taguchi, M. Hisakabe, and Y. Iwasa, Phys. Rev. Lett. **94**, 217002 (2005).
[17] T. Ekino, T. Takasaki, T. Muranaka, H. Fujii, J. Akimitsu, and S. Yamanaka, Physica B **328**, 23 (2003).
[18] Y. J. Uemura, Y. Fudamoto, I. M. Gat, M. I. Larkin, G. M. Luke, J. Merrin, K. M. Kojima, K. Itoh, S. Yamanaka, R. H. Heffner, and D. E. MacLaughlin, Physica B **289-290**, 389 (2000).
[19] A. Bill, H. Morawitz, and V. Z. Kresin, Phys. Rev. B **66**, 100501(R) (2002).
[20] Y. Taguchi, A. Kitora, and Y. Iwasa, Phys. Rev. Lett. **97**, 107001

(2006).
[21] H. Tou, Y. J. Tanaka, and S. Yamanaka (unpublished).
[22] N. R. Werthamer, E. Helfand, and P. C. Hohenberg, Phys. Rev. **147**, 295 (1966).
[23] J. J. Harris, J. A. Pals, and R. Woltjer, Rep. Prog. Phys. **52**, 1217 (1989).
[24] S. Komiya, H.-D. Chen, S.-C. Zhang, and Y. Ando, Phys. Rev. Lett. **94**, 207004 (2005).
[25] T. R. Chien, Z. Z. Wang, and N. P. Ong, Phys. Rev. Lett. **67**, 2088 (1991).
[26] H. Y. Hwang, B. Batlogg, H. Takagi, H. L. Kao, J. Kwo, R. J. Cava, J. J. Krajewski, and W. F. Peck, Phys. Rev. Lett. **72**, 2636 (1994).
[27] X. X. Zhang, C. Wan, H. Liu, Z. Q. Li, P. Sheng, and J. J. Lin, Phys. Rev. Lett. **86**, 5562 (2001).